Journal of Materials Chemistry C

PAPER

Cite this: J. Mater. Chem. C, 2015, 3, 2511

Fast fabrication of transparent and multi-luminescent TEMPO-oxidized nanofibrillated cellulose nanopaper functionalized with lanthanide complexes†

Miao Miao,[a] Jingpeng Zhao,[a] Xin Feng,*[a] Yang Cao,[c] Shaomei Cao,[a] Yafei Zhao,[a] Xiaoqian Ge,[a] Lining Sun,*[a] Liyi Shi[ab] and Jianhui Fang[b]

Received 17th November 2014
Accepted 14th January 2015

DOI: 10.1039/c4tc02622e

www.rsc.org/MaterialsC

We designed an easy-to-fabricate multi-luminescent nanopaper with high transparency, for the first time, by grafting lanthanide complexes [$Eu(dbm)_3(H_2O)_2$, $Sm(dbm)_3(H_2O)_2$, $Tb(tfacac)_3(H_2O)_2$] on TEMPO mediated oxidized nanofibrillated cellulose (ONFC). The lanthanide complex functionalized ONFC nanopaper (Ln–ONFC nanopaper, Ln = Eu, Sm, Tb) with uniform luminescence was rapidly fabricated after solvent exchange using a press-controlled extrusion papermaking method. The new TEMPO-induced carboxyl groups on the surface of ONFC provided the possibility to participate in the coordination with lanthanide ions and then to construct heterogeneous network architectures. The fluorescent properties of the Ln–ONFC hybrid nanopaper were significantly influenced by the amount of lanthanide complexes and the solvent medium during the extrusion. Based on simple manipulation and mild conditions, a highly transparent NFC template provided a soft matrix and afforded the high thermal stability and excellent luminescent properties of the Ln–ONFC nanopaper, which yields ever increasing potential to supersede petroleum-based materials for diverse applications.

1. Introduction

Traditionally, petroleum-based polymers have been extensively used due to their simple processing and low manufacturing costs.[1] However, most of them have larger coefficients of thermal expansion (CTE) than those of functional inorganic deposited materials, resulting in the invalidation of flexible devices under the condition of repeated bending or large changes in temperature. Nowadays, with the ever increasing consciousness for the global environment and energy sources, the utilization of eco-friendly and renewable native biopolymers are attracting extensive attention. Optical transparent nanopaper based on nanofibrillated cellulose (NFC) is emerging as a novel, environmentally friendly, biodegradable and renewable material, which could be the perfect candidate for plastic substrates in the future production of flexible electronics, such as solar cells, radio frequency identification (RFID) antennas, touch screens, chemical and biological sensors, organic field-effect transistors (OFETs) and a myriad of new flexible circuit technologies.[2–7] The biobased composition of NFC nanopaper is similar to that of traditional paper except that NFC nanopaper is made of nanocrystalline cellulose with a smaller diameter and higher crystallinity. As a result, NFC nanopaper exhibits excellent optical transmittance compared to regular cellulose paper. Furthermore, its low CTE (12–28.5 ppm K^{-1}), high tensile strength, enhanced printability and recyclability make it easy to process in higher temperatures than plastic substrates.[8–10]

Luminescent materials based on trivalent lanthanide ions have attracted much attention during the last decade. Luminescent lanthanide complexes display unique properties, including sharp emission peaks, high colour purity, long lifetimes and relative low toxicity,[11–14] making them promising in the fabrication of new types of anti-counterfeiting facilities, sensor systems and ion probes applications. NFC is an ideal building block to host a range of guest materials for NFC-based flexible matrices. Functionalized NFC hybrid nanopaper has attracted tremendous interest combined with exciting synergetic characteristics, including conductivity, fluorescence, magnetism, fire retardancy and gas barrier functions.[4–7,15–18] Recently, the synthesis and luminescent properties of inorganic quantum dots/cellulose, rare-earth complex/cellulose and their derivative nanocomposites have been reported.[19–23]

However, two issues, which need to be addressed for the fast fabrication of NFC hybrid nanopaper with homogenous

[a]Research Center of Nano Science and Technology, Shanghai University, Shanghai 200444, P. R. China. E-mail: fengxin@shu.edu.cn; lnsun@shu.edu.cn; Fax: +86-21-66136038; Tel: +86-21-66137257

[b]Department of Chemistry, Shanghai University, Shanghai 200444, P. R. China

[c]School of Materials Sciences and Engineering, Shanghai University, Shanghai 200444, P. R. China

† Electronic supplementary information (ESI) available. See DOI: 10.1039/c4tc02622e

network architectures still remain. First, for the incorporation of lanthanide complexes into the soft matrix, a problem often encountered by the physical doping method is the nonhomogeneous distribution of the complexes, which always leads to unavoidable agglomeration and a decrease of luminescence intensity. As an alternative, by covalently linking the complexes to the host matrix, a more homogeneous distribution of the lanthanide complex in the NFC network is formed, and this gives the possibility to achieve hybrid nanopaper. Second, for the fabrication of NFC nanopaper, the difficulty of extremely slow dewatering exists because of the high water binding capacity of NFC.[1,24,25] Traditionally, NFC nanopaper prepared using suspension-casting, water evaporation, and hot pressing to remove the excessive water is extremely time-consuming, and the procedures usually require several hours to a few days and even longer with complicated manipulations.[26–28] Sehaqui *et al.* reported that flat nanopaper was prepared in about 1 h using a semiautomatic sheet formed under vacuum.[29] Österberg *et al.* introduced overpressure filtration for the fast preparation of NFC films in less than 1 h, but there was always about 40% loss of material during filtration.[1]

Herein, a facile and highly efficient approach has been attempted to fabricate transparent and multi-luminescent nanopaper by the well dispersed 2,2,6,6-tetramethylpiperidinooxy (TEMPO) mediated oxidized NFC (ONFC) grafting with lanthanide complexes [$Eu(dbm)_3(H_2O)_2$, $Sm(dbm)_3(H_2O)_2$, $Tb(tfacac)_3(H_2O)_2$] using a pressure-controlled extrusion papermaking process. ONFC aqueous suspensions were treated with ethanol exchange to form a homogeneous solution with lanthanide complexes. The carboxyl groups on the surface of the ONFC participate in the covalent coupling process with lanthanide ions to form heterogeneous network architectures. The obtained Ln–ONFC hybrid nanopaper combines the advantages of both the lanthanide complexes and NFC nanopaper and exhibits synergetic properties. To the best of our knowledge, it is the first time lanthanide complex functionalized ONFC was synthesized by a coupling reaction for the easy fabrication of multi-luminescent nanopaper in less than 15 min, without adopting additional constraint clamping under vacuum to prevent wrinkling. Furthermore, the whole procedure is a simple operation, has mild reaction conditions and is environmentally-friendly.

2. Experimental section

2.1 Reagents and materials

1,1,1-Trifluoroacetylacetone (Htfacac, 99%, Alfa Aesar), and dibenzoylmethane (Hdbm, AR, Aladin) were used without further purification. Samarium oxide (Sm_2O_3, 99.99%), europium oxide (Eu_2O_3, 99.99%), and terbium oxide (Tb_4O_7, 99.99%) were bought from Sigma-Aldrich. Hydrated $LnCl_3$ salts (Ln = Eu, Sm, Tb) were obtained by dissolving Ln_2O_3 (Ln = Eu, Sm) or Tb_4O_7 in hydrochloric acid. The resulting solutions were evaporated with heating and the residues were dissolved in distilled water. 2,2,6,6-Tetramethyl-piperidinyl-1-oxyl (TEMPO, 98%) was purchased from Sigma Aldrich. Ethanol (AR, 95%), sodium bromide (NaBr, AR), and sodium hypochlorite (NaClO) were purchased from Sinopharm Chemical Reagent Co. Ltd (China) without further purification.

NFC aqueous suspensions were extracted after the chemical cleavage of the amorphous region of dealginate kelp residues by a high-pressure homogenization process (D–3L, PhD Technology LLC, USA).

The lanthanide complexes $Eu(dbm)_3(H_2O)_2$, $Sm(dbm)_3(H_2O)_2$, $Tb(tfacac)_3(H_2O)_2$) were synthesized according to the previously reported work.[30,31]

2.2 Preparation of TEMPO-mediated oxidized nanofibrillated cellulose (ONFC) ethanol suspension

ONFC was prepared according to a procedure previously described by Lin *et al.*[32] This method used TEMPO as a catalyst with a primary oxidant such as hypochlorite to oxidize the hydroxyl groups on the surface of NFC. Briefly, NFC aqueous suspensions were first treated by ultrasonic dispersion for 15 min. Then, the solution of TEMPO and NaBr in a given ratio was added successively. The oxidizing reaction was started by adding a certain amount of NaClO solution to the mixed dispersion, and the pH value was maintained at 10 by adding NaOH solution. After 3 h, the pH was adjusted to 7 with the addition of hydrochloric acid. Finally, the ONFC ethanol suspensions were prepared using a conventional solvent exchange process. ONFC aqueous suspensions were sonicated and centrifuged to remove the supernatant, and then the obtained filter cake was dispersed in ethanol with sonication and filtered again. This process was repeated five times and finally the filter cake was redispersed in ethanol to form a 0.03 wt% colloidal suspension.

2.3 Preparation of lanthanide complex grafted TEMPO-mediated oxidized nanofibrillated cellulose (Ln–ONFC) ethanol suspensions

Different amounts (5, 7.5, 10, 12 mg) of lanthanide complex $LnL_3(H_2O)_2$ (L = dbm, Ln = Eu, Sm; L = tfacac, Ln = Tb) was added in the 50 mL 0.03 wt% ONFC ethanol suspensions under stirring for 30 min, respectively. The resulting luminescent ONFC (Ln–ONFC, Ln = Eu, Sm, Tb) suspensions were obtained using the coupling reaction between $LnL_3(H_2O)_2$ and the carboxylate groups (–COONa) of the ONFC.

2.4 Preparation of luminescent Ln–ONFC hybrid nanopaper

The schematic diagram of the formation of Ln–ONFC nanopaper is shown in Scheme 1. The luminescent Ln–ONFC ethanol suspensions were poured into the extruder (NanoAble-150, PhD Technology LLC, USA) to remove ethanol with the controlled pressure of 0.6 MPa under N_2 gas, and nanopaper was formed on the filter membrane (PC, nuclepore track-etch membrane, pore size 100 nm, Whatman, UK) in less than 15 min. Then, the nanopaper was peeled off and sandwiched between two pieces of glass and dried in ambient atmosphere. Subsequently, transparent, flexible, and luminescent Ln–ONFC hybrid nanopaper with a 45 mm diameter and 30 μm thickness was finally fabricated.

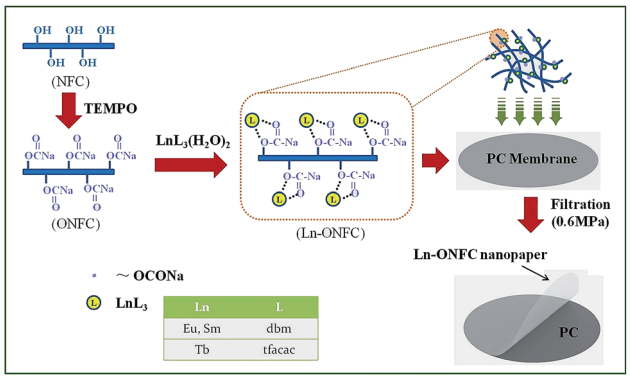

Scheme 1 Schematic diagram of the formation of Ln–ONFC hybrid nanopaper.

2.5 Preparation of Eu–ONFC–H_2O nanopaper

As a comparison, Eu–ONFC–H_2O nanopaper was prepared with aqueous suspensions other than ethanol suspensions using a similar extrusion paper-making method.

2.6 Preparation of pure NFC and ONFC nanopaper

As a comparison, pure NFC nanopaper was synthesized without TEMPO oxidation and the addition of lanthanide complexes, and pure ONFC nanopaper was also synthesized without the addition of lanthanide complexes, using a similar extrusion paper-making method.

2.7 Characterization

The structure of the nanopaper was characterized through Fourier transform infrared spectroscopy (FTIR, AVATAR370, USA) with the spectral width ranging from 4000 to 400 cm^{-1} by grinding KBr as transparent pellets. Surface morphologies were examined by scanning electron microscopy (SEM, JSM-6700F, JEOL, Japan). The optical properties were measured on a UV-vis spectrophotometer (UV-2501PC, Shimadzu, Japan). The excitation and emission spectra were measured with a spectrofluorophotometer (RF-5301PC, Shimadzu, Japan; FLS-920, Edinburgh, UK). The thermal stability was investigated by a thermogravimetric analyzer (TGA, STA409PC, Netzsch, Germany). The thickness of the samples was measured three times with a paper thickness meter (PT-4A, China).

3. Results and discussion

The FTIR spectra of pure NFC nanopaper, ONFC nanopaper and Eu-ONFC nanopaper are shown in Fig. 1. The characteristic signals located at 3417 cm^{-1} and 2901 cm^{-1} are attributed to the stretching vibration of –OH groups and stretching vibrations of C–H, respectively.[33] Upon the TEMPO oxidation, the important change for ONFC and Eu-ONFC is the appearance of the carboxyl groups (C=O) resulting from the surface sodium carboxylate groups (–COONa). In the spectrum of ONFC nanopaper, carboxyl groups (C=O) were hardly observed due to the interference of the absorbed water band (1636 cm^{-1}).[32] To

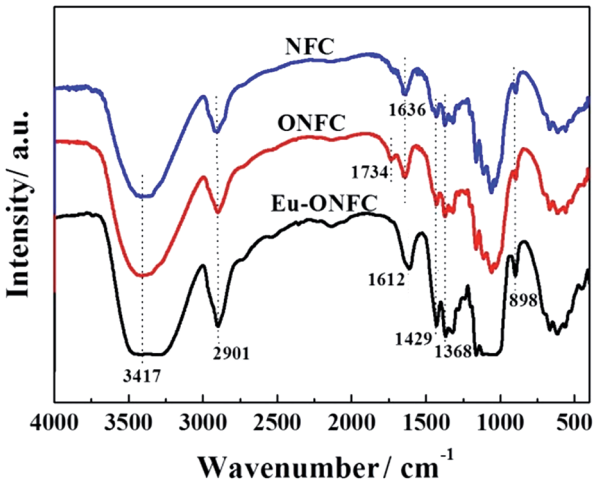

Fig. 1 FTIR spectra of pure NFC nanopaper, ONFC nanopaper and Eu–ONFC nanopaper.

clearly observe the change from the oxidation, ONFC nanopaper was treated by HCl solution according to the previous literature.[32] –COONa was converted to the acidic form –COOH under an ion exchange procedure. The carboxyl groups (C=O) stretching vibration at 1734 cm^{-1} is clearly shown and is ascribed to –COOH. After the immobilization of $Eu(dbm)_3(H_2O)_2$ on ONFC, the new peak located at 1612 cm^{-1} was assigned to the strong stretching vibration of carboxylate,[32] suggesting the coupling reaction between ONFC and $Eu(dbm)_3(H_2O)_2$.[34] The FT-IR spectra of the other Ln–ONFC (Ln = Tb, Sm) nanopapers are very similar to that of Eu–ONFC. Therefore, the FTIR results demonstrated that the $LnL_3(H_2O)_2$ (L = dbm, Ln = Eu, Sm; L = tfacac, Ln = Tb) were covalently bonded with ONFC, resulting in the formation of Ln–ONFC nanopaper.

The luminescence properties of the Eu–ONFC nanopaper were investigated by fluorescence spectroscopy. Fig. 2 shows the

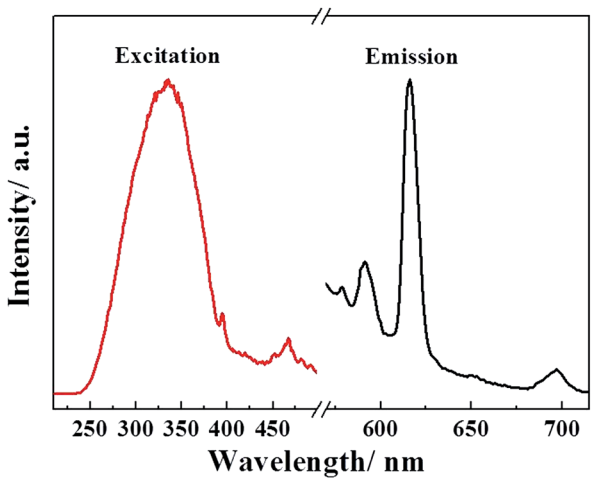

Fig. 2 Excitation and emission spectra of Eu–ONFC nanopaper with 10 mg $Eu(dbm)_3(H_2O)_2$.

excitation and emission spectra of the Eu–ONFC nanopaper. The excitation spectrum was obtained by monitoring the strongest emission of Eu^{3+} at 616 nm. A broad band in the UV/visible region ranging from 250 to 400 nm can be observed, which is attributed to the absorption of organic ligands (dbm and ONFC). Under excitation at 336 nm, the characteristic emission bands at 579 nm, 591 nm, 616 nm, 650 nm and 697 nm of Eu–ONFC nanopaper can be assigned to the $^5D_0 \rightarrow {}^7F_J$ (J = 0, 1, 2, 3 and 4) transitions of Eu^{3+} ion. The $^5D_0 \rightarrow {}^7F_2$ transition at 616 nm is the strongest emission, which is an induced electric dipole transition and is responsible for the brilliant red emission of Eu–ONFC nanopaper.[35] It can be deduced that the dbm and ONFC ligands are able to transfer the absorbed UV energy to the Eu^{3+} ion *via* the antenna effect and the corresponding Eu complexes are formed between the Eu^{3+} ion and the ligands in Eu–ONFC nanopaper. The emission spectra of the Eu–ONFC nanopaper with different amounts of $Eu(dbm)_3(H_2O)_2$ complexes (0–12 mg) is shown in Fig. S1.† It can be observed that the emission intensity was gradually enhanced when the amount of $Eu(dbm)_3(H_2O)_2$ complexes increased. Then, it is reasonable to deduce that in a qualitatively way, no quenching effects were detected with increasing the amount of lanthanide complexes from 0 to 12 mg, as the experimental conditions (such as excitation power and detection slits) were kept constant during the entire set of measurements.

The distribution and morphologies of the lanthanide complex would play a critical role on the optical transmittance and luminescence properties of the nanopaper, which contains the lanthanide complex.[6,19,36] The SEM images of the luminescent Eu–ONFC nanopaper with different dosages of 5 mg, 7.5 mg, 10 mg and 12 mg $Eu(dbm)_3(H_2O)_2$ are shown in Fig. 3, respectively. It can be noted that all of the Eu–ONFC nanopapers exhibited a compact and uniform fibrous network structure assembled with the NFC template. With the increase of the $Eu(dbm)_3(H_2O)_2$ concentration to 10 mg in the initial ethanol suspension, the relatively smooth surface of the Eu–ONFC nanopaper can be preserved (Fig. 3a–c). However, an increased amount of $Eu(dbm)_3(H_2O)_2$ (12 mg) would inevitably result in the rough and lumpy surface of the nanopaper (Fig. S2†). In addition, when the amount of $Eu(dbm)_3(H_2O)_2$ is about 10 mg, a uniform red emission can be obtained under excitation with UV light at 365 nm (inset of Fig. 3c). The increase of $Eu(dbm)_3(H_2O)_2$ concentration will result in the reduction of the uniformity of the heterogeneous network architectures of the Eu–ONFC nanopaper. The lower loading of $Eu(dbm)_3(H_2O)_2$ will be followed with a relatively decreasing luminescent intensity of the Eu–ONFC nanopaper. Taking into account the results mentioned above, an optimum lanthanide complex amount (10 mg) can be employed to synthesize the Ln–ONFC (Ln = Sm, Tb) nanopaper with a high loading of the lanthanide complex and a uniform heterogeneous network architecture can still be obtained.

When the ethanol solvent was replaced by H_2O during the synthesis of the nanopaper, the resulting Eu–ONFC–H_2O nanopaper (with 10 mg $Eu(dbm)_3(H_2O)_2$) shows a highly rough surface (Fig. 3d) and non uniform luminescence (inset of Fig. 3d). Therefore, the kind of solvent plays an important role in the synthesis of uniform luminescent nanopaper. For the Eu–ONFC–H_2O nanopaper, this may be due to the hydrophobic property of the lanthanide complex $Eu(dbm)_3(H_2O)_2$ in aqueous media, which causes inadequate linking and poor compatibility with ONFC. The coordination of $Eu(dbm)_3(H_2O)_2$ and ONFC in water leads to an inhomogeneous distribution and aggregation of the Eu complex, resulting in the irregular surface and non uniform luminescence of the Eu–ONFC–H_2O nanopaper.

The optical transparency of the nanopaper was investigated, as shown in Fig. 4. As the diameters of the NFC and ONFC are in the range of 10–20 nm (Fig. S3†), the light scattering effect is significantly reduced and most of the light propagates through the nanopaper.[6] Thus, both ONFC and the Eu–ONFC nanopaper

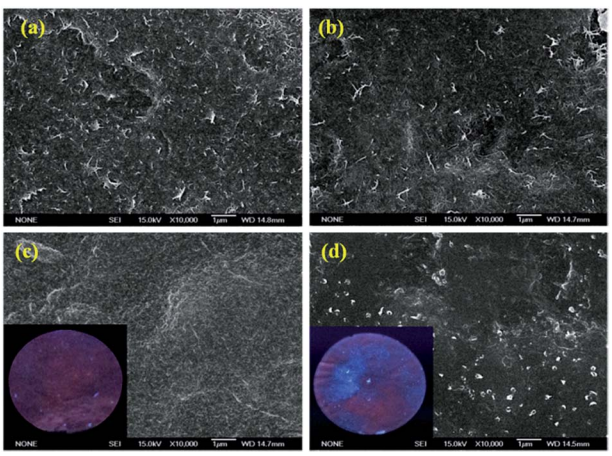

Fig. 3 Typical SEM images of the luminescent Eu–ONFC nanopaper with different $Eu(dbm)_3(H_2O)_2$ contents: 5 mg (a), 7.5 mg (b) and 10 mg (c). SEM image of Eu–ONFC–H_2O nanopaper prepared by H_2O as the solvent with the optimal dosage of 10 mg (d). Insets in (c and d): the emission images of nanopaper under excitation with UV light (365 nm).

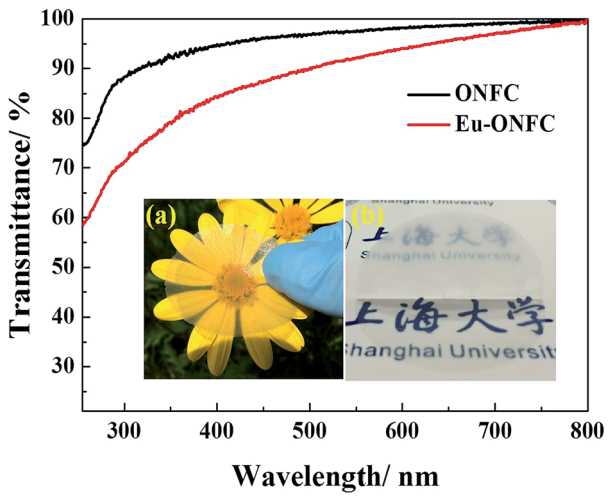

Fig. 4 Optical transmittance curves of ONFC nanopaper and Eu–ONFC nanopaper with 10 mg $Eu(dbm)_3(H_2O)_2$. Inset: the images of transparent (a) and foldable (b) Eu–ONFC nanopaper.

display very high transmittance in comparison with the previously reported nanopaper.[29,37] Compared with the ONFC nanopaper, the light transmittance of the Eu–ONFC nanopaper decreased slightly from 94% to 84% at the wavelength of 400 nm, which is probably attributed to the light absorption of the lanthanide complex and the light scattering of the relatively rough nanopaper. The transparent and foldable properties of the resulting Eu–ONFC nanopaper can be further demonstrated from the inset pictures. Fig. 4a shows the picture of the Eu–ONFC nanopaper with close contact to a flower, displaying high optical transparency. As shown in Fig. 4b, the Eu–ONFC nanopaper is as foldable as conventional paper. Through the transparent and luminescent Eu–ONFC nanopaper, the school emblem of Shanghai University on the background can be clearly identified, whereas the school emblem behind the folded part becomes fuzzy, which is attributed to the large light scattering effect of the incident light.[6,38] Therefore, the flexibility, unique optical transparency and haze of luminescent Eu–ONFC nanopaper would expand their usage for applications in anti-glare, wearability and portability, *etc.*

Encouraged by the excellent transparency and luminescent property of the Eu–ONFC nanopaper and the efficient synthetic method, Sm–ONFC nanopaper and Tb–ONFC nanopaper were also synthesized using a similar method except that $Eu(dbm)_3(H_2O)_2$ was replaced by $Sm(dbm)_3(H_2O)_2$ and $Tb(tfacac)_3(H_2O)_2$ with the optimal dosage of 10 mg, respectively. Fig. 5 reveals the SEM morphologies of Sm–ONFC nanopaper and Tb–ONFC nanopaper. It can be noted that both the Sm–ONFC nanopaper and Tb–ONFC nanopaper show smooth surface morphologies with uniform distribution of the numerous interconnected ONFC, which are similar with that of the Eu–ONFC nanopaper. The result indicates that different lanthanide complexes have no obvious effect on the morphology of Ln–ONFC nanopaper.

The excitation and emission spectra of the Sm–ONFC nanopaper and Tb–ONFC nanopaper are displayed in Fig. 6, respectively. As shown in Fig. 6a, the excitation spectrum of Sm–ONFC nanopaper, measured by monitoring the strongest emission of Sm^{3+} at 650 nm, displays a broad band ranging from 320 to 450 nm, which is attributed to the absorption of the ligands. In the visible emission spectrum of the Sm–ONFC nanopaper (λ_{ex} = 380 nm), the strongest emission can be observed at 650 nm, which is due to the $^4G_{5/2} \rightarrow {}^6H_{9/2}$ transition of the Sm^{3+} ion.[14] It is found that Sm–ONFC nanopaper displays

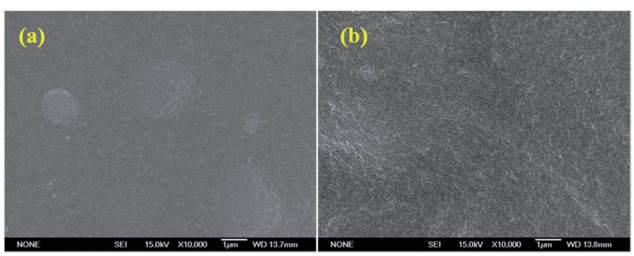

Fig. 5 Typical SEM morphologies of the Sm–ONFC nanopaper (a) and Tb–ONFC nanopaper (b).

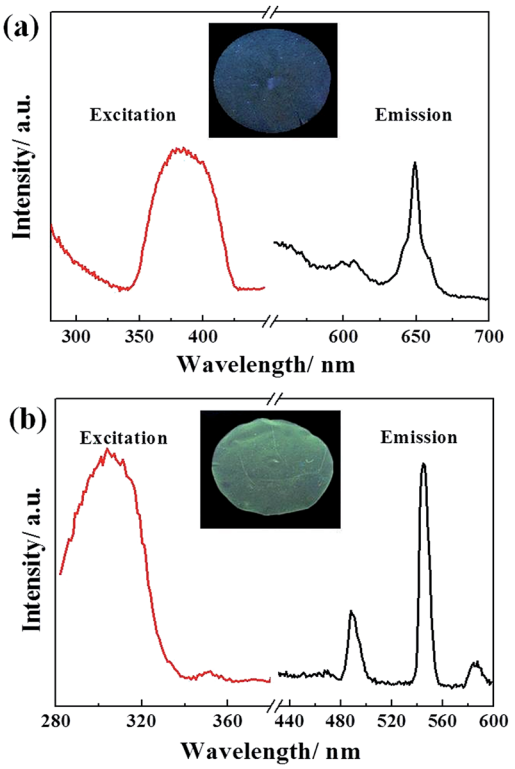

Fig. 6 Excitation and emission spectra of (a) Sm–ONFC nanopaper and (b) Tb–ONFC nanopaper. Inset: images of Sm–ONFC nanopaper excited with UV light at 365 nm (a) and Tb–ONFC nanopaper excited with UV light at 254 nm (b).

orange luminescence upon UV excitation at 365 nm (inset in Fig. 6a). The excitation spectrum of Tb–ONFC nanopaper (Fig. 6b) was obtained by monitoring the strongest emission of the Tb^{3+} ion (λ_{em} = 545 nm). The spectrum exhibits a broad band in the UV region, which is due to the absorption of the tfacac and ONFC ligands. Upon excitation at 304 nm, the emission spectrum of the Tb–ONFC nanopaper shows the characteristic luminescence of the Tb^{3+} ion, located at 488 nm ($^5D_4 \rightarrow {}^7F_6$), 545 nm ($^5D_4 \rightarrow {}^7F_5$), and 582 nm ($^5D_4 \rightarrow {}^7F_4$), in which the $^5D_4 \rightarrow {}^7F_5$ transition is the most prominent one. Upon UV light illumination (254 nm), the Tb–ONFC nanopaper displays green luminescence, which can be easily detected by the naked eye (inset in Fig. 6b).[39] As described above, the visible luminescence of lanthanide ions was obtained in the corresponding Ln–ONFC nanopaper (Ln = Eu, Sm, Tb) following the excitation of the absorption of their organic ligands. Thus, it is obvious that the intramolecular energy transfer does happen between the ligands and the Ln^{3+} ions. Therefore, it is reasonable to conclude that the ternary lanthanide complexes are bonded to ONFC.

The thermal stability of the ONFC hybrid nanopaper is another important parameter to pave the way for a variety of useful applications as biopolymer substrates or inter-spacing layers. It has been demonstrated that nanopaper has a much lower CTE than glass and plastic,[9,10] suggesting its better capability to tolerate large changes in temperature. The thermal

stability of the Ln–ONFC nanopaper (Ln = Eu, Sm, Tb) was investigated by TG analysis. The TG profiles of the Ln–ONFC nanopaper are very similar, and the Eu–ONFC nanopaper is given as a representative. As shown in Fig. 7, the TGA curves of the ONFC nanopaper and Eu–ONFC nanopaper both exhibit three stages of weight loss. The first stage from the range of 20 °C to 220 °C with a small weight loss is due to the evaporation of water or decomposition of some micromolecules. At the second stage from 220 °C to 370 °C, cellulose undergoes the processes of depolymerisation, dehydration and decomposition of its glycoside units with the main weight loss of 57% for ONFC and 62% for Eu–ONFC. The third stage happens because of the degradation of the charred residues to form gaseous products of low molecular weight. In the first two stages, the degradation temperature of the Eu–ONFC nanopaper was very close to that of pure ONFC nanopaper, while a little difference can be observed in the third stage. Eu–ONFC nanopaper presents more carbonized residues than ONFC, which is probably related to the introduction of lanthanide complex acting as flame retardants. The excellent property of thermal stability for the Ln–ONFC nanopaper gives the possibility to replace other film materials for wide applications.

In addition, the potential application of Ln–ONFC nanopaper to be used for security printing was investigated. Quick response (QR) codes of about 25 mm × 25 mm were directly printed on the surface of the Tb–ONFC nanopaper using a colorless carbon dots (CD) aqueous solution as the printing ink. The CD aqueous solution obtained according to the previous report,[40] has optimal excitation and emission peaks at 360 nm and 443 nm, respectively. Fig. 8 shows the digital pictures of the as-prepared Tb–ONFC nanopaper printed QR codes under daylight and UV light, respectively. It is obvious that the Tb–ONFC nanopaper printed with QR codes maintains high transparency, and the QR codes are invisible under daylight (Fig. 8a); however, the anticipated blue luminescent QR codes appear under UV light excitation at 365 nm, as shown in Fig. 8b. Remarkably, when excited with UV light at 254 nm, green luminescent Tb–ONFC nanopaper and blue luminescent QR codes can be simultaneously observed. Therefore, the excellent "visible–invisible" and "UV-visible" properties of Ln–ONFC nanopaper printed with CD ink can be easily applied for anti-counterfeiting and labelling fields,[41] and the synergic features of transparency and multi-luminescence further strengthens the extensibility and fidelity in multiple anti-counterfeiting technologies for documents and products.

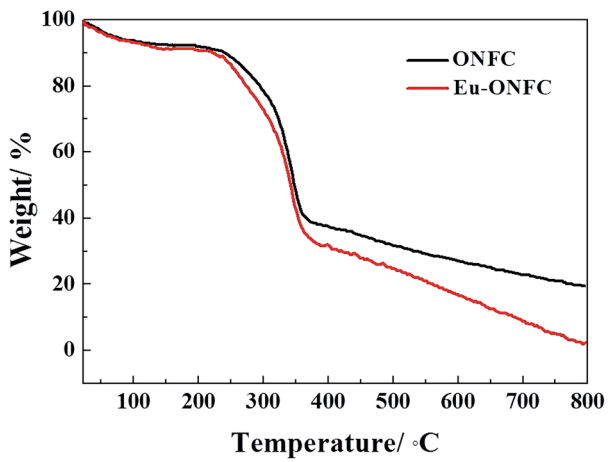

Fig. 7 TGA profiles of ONFC nanopaper and Eu–ONFC nanopaper with 10 mg $Eu(dbm)_3(H_2O)_2$.

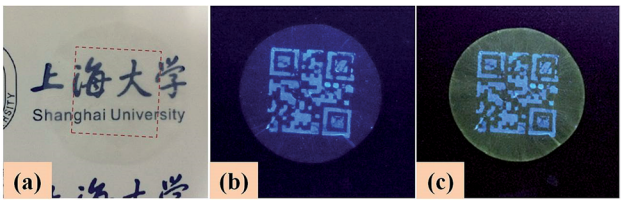

Fig. 8 Images of Tb–ONFC nanopaper printed with QR codes by CD ink under daylight (a) and UV light at 365 nm (b) and 254 nm (c). The red dashed box of (a) marks the location of the QR codes.

4. Conclusions

A fast press-controlled extrusion paper-making process has been used for three kinds of lanthanide complex functionalized ONFC hybrid nanopaper with high transparency, for the first time. In the nanopaper-making process, a simple solvent exchange and subsequently fast extrusion procedure were included. Through the systematic and comparative study of the Eu–ONFC nanopaper with different amounts of $Eu(dbm)_3(H_2O)_2$, the optimum lanthanide complex amount (10 mg) was selected as the candidate condition for the preparation of Ln–ONFC (Ln = Eu, Sm, Tb) nanopaper. The three Ln–ONFC (Ln = Eu, Sm, Tb) nanopapers show good flexibility, unique optical transparency, and good thermal stability. Of importance is that after ligand-mediated excitation, the emission spectra of the Ln–ONFC (Ln = Eu, Sm, Tb) nanopaper all show the characteristic luminescence of the corresponding lanthanide ions through the intramolecular energy transfer from the ligands to the lanthanide ions, indicating that the lanthanide complexes are formed and covalently linked to the ONFC network. The excellent properties and uniform luminescence (red for Eu–ONFC, orange for Sm–ONFC, and green for Tb–ONFC) of the Ln–ONFC nanopaper offer advantages including ease of synthesis and handling as well as potential applications for the anti-counterfeiting and labelling fields, and marking soft materials, which serve for ID-card and credit card protection and other security applications.

Acknowledgements

This work was financially supported by the Science and Technology Commission of Shanghai Municipality (13ZR1415100, 15ZR1415100, 13JC1402700, 13NM1401101, 14520722200), the National Natural Science Foundation of China (Grant no. 21231004), Innovation Program of Shanghai Municipal Education Commission (13ZZ073), Shanghai Foundation of Excellent Young University Teacher, and Shanghai Rising-Star Program

(14QA1401800). The authors are also grateful to Instrumental Analysis & Research Center of Shanghai University.

Notes and references

1 M. Österberg, J. Vartiainen, J. Lucenius, U. Hippi, J. Seppälä, R. Serimaa and J. Laine, *ACS Appl. Mater. Interfaces*, 2013, **5**, 4640.

2 H. L. Zhu, B. B. Narakathu, Z. Q. Fang, A. T. Aijazi, M. Joyce, M. Atashbar and L. Hu, *Nanoscale*, 2014, **6**, 9110.

3 T. S. Kim, S. I. Na, S. S. Kim, B. K. Yu, J. S. Yeo and D. Y. Kim, *Phys. Status Solidi RRL*, 2012, **6**, 13.

4 B. Wang and L. L. Kerr, *Sol. Energy Mater. Sol. Cells*, 2011, **95**, 2531.

5 M. C. Barr, J. A. Rowehl, R. R. Lunt, J. Xu, A. Wang, C. M. Boyce, S. G. Im, V. Bulović and K. K. Gleason, *Adv. Mater.*, 2011, **23**, 3500.

6 L. B. Hu, G. Y. Zheng, J. Yao, N. Liu, B. Weil, M. Eskilsson, E. Karabulut, Z. Ruan, S. Fan, J. T. Bloking, M. D. McGehee, L. Wågberg and Y. Cui, *Energy Environ. Sci.*, 2013, **6**, 513.

7 J. W. Han, B. Kim, J. Li and M. Meyyappan, *J. Phys. Chem. C*, 2012, **116**, 22094.

8 H. L. Zhu, Z. Q. Fang, C. Preston, Y. Y. Li and L. B. Hu, *Energy Environ. Sci.*, 2014, **7**, 269.

9 R. J. Moon, A. Martini, J. Nairn, J. Simonsen and J. Youngblood, *Chem. Soc. Rev.*, 2011, **40**, 3941.

10 J. Huang, H. L. Zhu, Y. C. Chen, C. Preston, K. Rohrbach, J. Cumings and L. B. Hu, *ACS Nano*, 2013, **7**, 2106.

11 J. C. G. Bünzli and C. Piguet, *Chem. Soc. Rev.*, 2005, **34**, 1048.

12 J. C. G. Bünzli, *Acc. Chem. Res.*, 2006, **39**, 53.

13 L. N. Sun, W. P. Mai, S. Dang, Y. N. Qiu, W. Deng, L. Y. Shi, W. Yan and H. J. Zhang, *J. Mater. Chem.*, 2012, **22**, 5121.

14 L. N. Sun, Y. N. Qiu, T. Liu, J. Z. Zhang, S. Dang, J. Feng, Z. J. Wang, H. J. Zhang and L. Y. Shi, *ACS Appl. Mater. Interfaces*, 2013, **5**, 9585.

15 H. L. Zhu, S. Parvinian, C. Preston, O. Vaaland, Z. C. Ruan and L. B. Hu, *Nanoscale*, 2013, **5**, 3787.

16 R. T. Olsson, M. A. S. Azizi Samir, G. Salazar-Alvarez, L. Belova, V. Ström, L. A. Berglund, O. Ikkala, J. Nogrés and U. W. Gedde, *Nat. Nanotechnol.*, 2010, **5**, 584.

17 A. D. Liu, A. Walther, O. Ikkala, L. Belova and L. A. Berglund, *Biomacromolecules*, 2011, **12**, 633.

18 J. P. Zhao, Z. W. Wei, X. Feng, M. Miao, L. N. Sun, S. M. Cao, L. Y. Shi and J. H. Fang, *ACS Appl. Mater. Interfaces*, 2014, **6**, 14945.

19 J. S. Huo, Y. H. Zheng, S. T. Pang and Q. M. Wang, *Cellulose*, 2013, **20**, 841.

20 Z. H. Yang, S. Y. Chen, W. L. Hu, N. Yin, W. Zhang, C. Xiang and H. P. Wang, *Carbohydr. Polym.*, 2012, **88**, 173.

21 P. Kulpinski, A. Erdman, M. Namyslak and J. D. Fidelus, *Cellulose*, 2012, **19**, 1259.

22 P. Kulpinski, M. Namyslak, T. Grzyb and S. Lis, *Cellulose*, 2012, **19**, 1271.

23 H. Q. Wang, Z. Q. Shao, M. Bacher, F. Liebne and T. Rosenau, *Cellulose*, 2013, **20**, 3007.

24 K. Junka, J. Guo, I. Filpponen, J. Laine and O. J. Rojas, *Biomacromolecules*, 2014, **15**, 876.

25 W. Y. Huang, X. L. Ouyang and L. J. Lee, *ACS Nano*, 2012, **6**, 10178.

26 M. Nogi, S. Iwamoto, A. N. Nakagaito and H. Yano, *Adv. Mater.*, 2009, **21**, 1595.

27 T. Zimmermann, E. Pohler and T. Geiger, *Adv. Energy Mater.*, 2004, **6**, 754.

28 M. E. Malainine, M. Mahrouz and A. Dufresne, *Compos. Sci. Technol.*, 2005, **65**, 1520.

29 H. Sehaqui, A. Liu, Q. Zhou and L. A. Berglund, *Biomacromolecules*, 2010, **11**, 2195.

30 L. N. Sun, H. J. Zhang, C. Y. Peng, J. B. Yu, Q. G. Meng, L. S. Fu, F. Y. Liu and X. M. Guo, *J. Phys. Chem. B*, 2006, **110**, 7249.

31 C. R. D. Silva, J. Li, Z. P. Zheng and L. R. Corrales, *J. Phys. Chem. A*, 2008, **112**, 4527.

32 N. Lin, C. Bruzzese and A. Dufresne, *ACS Appl. Mater. Interfaces*, 2012, **4**, 4948.

33 C. Y. Chang, J. Peng, L. N. Zhang and D. W. Pang, *J. Mater. Chem.*, 2009, **19**, 7771.

34 Z. Zhou and Q. M. Wang, *Sens. Actuators, B*, 2012, **173**, 833.

35 L. N. Sun, Z. J. Wang, J. Z. Zhang, J. Feng, J. L. Liu, Y. Zhao and L. Y. Shi, *RSC Adv.*, 2014, **4**, 28481.

36 M. Surin, E. Hennebicq, C. Ego, D. Marsitzky, A. C. Grimsdale, K. Müllen, J. L. Brédas, R. Lazzaroni and P. Leclère, *Chem. Mater.*, 2004, **16**, 994.

37 H. Sehaqui, N. E. Mushi, S. Morimune, M. Salajkova, T. Nishino and L. A. Berglund, *ACS Appl. Mater. Interfaces*, 2012, **4**, 1043.

38 Z. Q. Fang, H. L. Zhu, C. Preston, X. G. Han, Y. Y. Li, S. Lee, X. S. Chai, G. Chen and L. B. Hu, *J. Mater. Chem. C*, 2013, **1**, 6191–6197.

39 L. N. Sun, J. B. Yu, H. S. Peng, J. Z. Zhang, L. Y. Shi and O. S. Wolfbeis, *J. Phys. Chem. C*, 2010, **114**, 12642.

40 S. Zhu, Q. Meng, L. Wang, J. Zhang, Y. Song, H. Jin, K. Zhang, H. Sun, H. Wang and B. Yang, *Angew. Chem.*, 2013, **125**, 4045.

41 S. S Liu, C. F Wang, C. X. Li, J. Wang, L. H. Mao and S. Chen, *J. Mater. Chem. C*, 2014, **2**, 6477.